Proc. 12th Int. Conf. Low Energy Antiproton Physics (LEAP2016)
JPS Conf. Proc. **18**, 011018 (2017)
https://doi.org/10.7566/JPSCP.18.011018

Towards an Improved Measurement of the Proton Magnetic Moment

Georg Schneider[1,2], Nathan Leefer[3], Andreas Mooser[2], Klaus Blaum[4], Takashi Higuchi[2,5], Yasuyuki Matsuda[5], Hiroki Nagahama[2,5], Wolfgang Quint[6], Stefan Sellner[2], Christian Smorra[2,7], Jochen Walz[1,3], and Stefan Ulmer[2]

[1]*Institut für Physik, Johannes Gutenberg-Universität Mainz, 55099 Mainz, Germany*
[2]*Ulmer Initiative Research Unit, RIKEN, Saitama 351-0198, Japan*
[3]*Helmholtz-Institut Mainz, 55099 Mainz, Germany*
[4]*Max-Planck-Institut für Kernphysik, 69117 Heidelberg, Germany*
[5]*Graduate School of Arts and Sciences, University of Tokyo, Tokyo 153-8902, Japan*
[6]*GSI-Helmholtzzentrum für Schwerionenforschung, 64291 Darmstadt, Germany*
[7]*CERN, 1211 Geneva 23, Switzerland*

E-mail: georg.schneider@uni-mainz.de

(Received May 24, 2016)

The BASE collaboration performed the most precise measurement of the proton magnetic moment. By applying the so-called double Penning-trap method with a single proton a fractional precision of 3.3 parts-per-billion was reached. This article describes the primary limitations of the last measurement and discusses improvements to reach the sub-parts-per-billion level.

KEYWORDS: proton, antiproton, magnetic moment, g-factor, double trap method, CPT, Penning trap

1. Introduction

Invariance under the combined transformation of charge (C), parity (P), and time (T) is an exact symmetry of the relativistic quantum field theories involved in the Standard Model of particle physics. Consequently the fundamental properties of matter and antimatter conjugates are predicted to be identical, apart from signs. On cosmological scales, on the other hand, a dominance of matter over antimatter is observed.

This unexplained imbalance between antimatter and matter provides a strong motivation for the experiments of the BASE collaboration [1, 2] which contribute to stringent CPT tests by comparing the fundamental properties of protons and antiprotons, in particular charge-to-mass ratios $(q/m)_\mathrm{p}/(q/m)_{\bar{\mathrm{p}}}$ and magnetic moments $\mu_{\mathrm{p},\bar{\mathrm{p}}} = g_{\mathrm{p},\bar{\mathrm{p}}}/2 \cdot \mu_\mathrm{N}$, where $\mu_\mathrm{N} = q\hbar/(2m_{\mathrm{p},\bar{\mathrm{p}}})$ is the nuclear magneton with charge q and the mass m of the proton/antiproton, respectively. In 2014 we measured the g-factor of a single trapped proton with a fractional precision of 3.3 parts-per-billion (p.p.b.) [3]

$$g_\mathrm{p} = 5.585\,694\,700(14)^{\mathrm{stat}}(12)^{\mathrm{syst}}\,. \tag{1}$$

Our measurement improved the 42 year old MASER based value [4] by a factor of 2.5 and is the most precise direct measurement of g_p.

The experiment was carried out by applying the double Penning-trap method [5]. The g-factor is obtained by measuring the ratio of the particle's free cyclotron frequency $\nu_\mathrm{c} = 1/(2\pi)\, q/m\, B_0$ and its spin precession frequency $\nu_\mathrm{L} = g_\mathrm{p}/2 \cdot \nu_\mathrm{c}$, the Larmor frequency. The precision frequency measurements are carried out in a "precision trap" with homogeneous magnetic field, while the spin state analysis, essential for the Larmor frequency determination, is conducted in an "analysis trap"

with a strong superimposed magnetic inhomogeneity [6]. The fractional precision achieved in these measurements was limited by the residual magnetic field inhomogeneity in the precision trap and by nonlinear magnetic field drifts. Both contributed to a broadening of the measured g-factor resonance and led to systematic shifts [3]. In this article we discuss the previous limitations and describe the implementation of experimental improvements which will allow an order of magnitude increase in precision for the measured g-factor.

2. Penning trap and frequency detection

Our experiment makes use of two cylindrical Penning traps which consist of five electrodes [7] and a superimposed magnetic field, see Fig. 1. Dimensions of the electrodes and applied voltages are chosen such that an ideal quadrupole potential is realized in the center of the trap. The trajectory of a

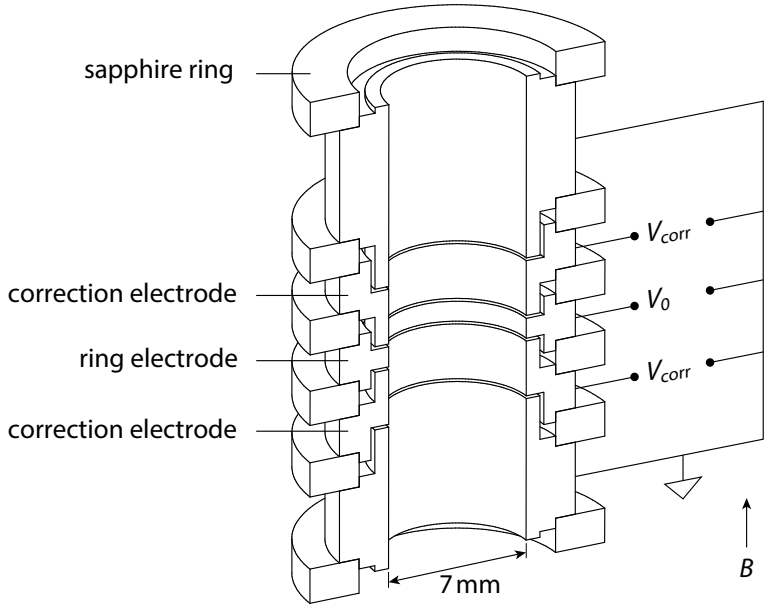

Fig. 1. Schematic cylindrical Penning trap with characteristic voltages on five trap electrodes. The gold-plated copper electrodes are separated by sapphire rings. The ring voltage V_0 and the correction voltage V_{corr} lead to a quadrupole field in the trap center. This static electric field together with a superimposed magnetic field allows stable storage of charged particles.

single particle in such a Penning trap is described by the superposition of three independent harmonic oscillator motions [8], the axial motion as a result of the electrostatic potential at

$$\nu_z = \frac{1}{2\pi}\sqrt{\frac{2qC_2V_0}{m}}, \tag{2}$$

where V_0 is the voltage on the ring electrode and C_2 is a trap specific geometric parameter, the modified cyclotron motion at

$$\nu_+ = \frac{1}{2}\left(\nu_c + \sqrt{\nu_c^2 - 2\nu_z^2}\right), \tag{3}$$

and the magnetron motion with frequency

$$\nu_- = \frac{1}{2}\left(\nu_c - \sqrt{\nu_c^2 - 2\nu_z^2}\right), \tag{4}$$

due to the $\boldsymbol{E} \times \boldsymbol{B}$ drift of the particle.

The invariance theorem [9] allows the determination of the free cyclotron frequency ν_c by measurement of ν_+, ν_z, and ν_-

$$\nu_c = \sqrt{\nu_+^2 + \nu_z^2 + \nu_-^2} \, . \tag{5}$$

The axial frequency ν_z of the particle can be measured by applying a non-destructive image current detection technique. The particle induces small image currents on the order of a few femto-Ampere which are detected with a tuned superconducting LC circuit, the axial detector. The detector acts like a thermal bath that cools the particle resistively. In thermal equilibrium the particle shorts the Johnson-Nyquist noise of the detector and appears as a dip at ν_z in the fast Fourier transform (FFT) spectrum of the detector's time signal. This is shown in Fig. 2. (a).

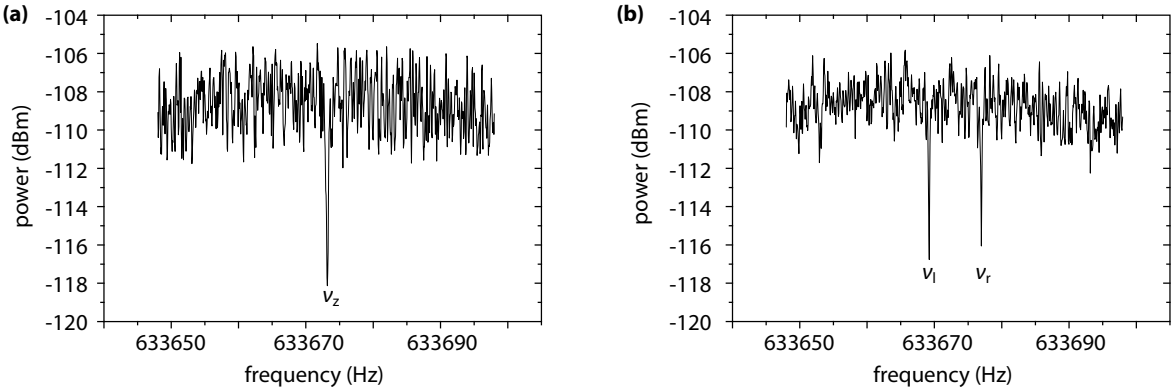

Fig. 2. (a) In thermal equilibrium the proton shorts the Johnson-Nyquist noise of the axial detector which results in a single dip in the FFT spectrum. (b) A rf-drive is applied to one of the trap electrodes which couples the modified cyclotron mode to the axial mode. As a result a double-dip can be observed. From the combined measurements of both the single and the double-dip, the modified cyclotron frequency can be determined.

The modified cyclotron frequency ν_+ and the magnetron frequency ν_- are also measured with the axial detector by using sideband coupling [8]. A quadrupole radiofrequency (rf) drive at approximately $\nu_{rf} = \nu_z + \nu_-$ (or $\nu_{rf} = \nu_+ - \nu_z$) is applied to the trap electrodes, which leads to a coupling of the axial mode to the magnetron or cyclotron mode, respectively. As a result the single dip at ν_z splits into a double-dip ν_r and ν_l as shown in Fig. 2. (b) for the modified cyclotron mode. ν_+ can be calculated with the measurement of the frequencies ν_r, ν_l and the axial frequency ν_z from an independent single dip measurement

$$\nu_+ = \nu_l + \nu_r + \nu_{rf} - \nu_z \, , \tag{6}$$

and likewise for the magnetron frequency ν_-

$$\nu_- = -\nu_l - \nu_r + \nu_{rf} + \nu_z \, . \tag{7}$$

Mode coupling is not only crucial for frequency measurements but also for changing the particle's energy. While the coupling drive is applied, energy is exchanged between the modes and an equilibrium is reached with $\langle n_z \rangle = \langle n_\pm \rangle$ [8]. This leads to

$$\langle E_- \rangle = \frac{\nu_-}{\nu_z} \langle E_z \rangle \quad \text{and} \quad \langle E_+ \rangle = \frac{\nu_+}{\nu_z} \langle E_z \rangle \, . \tag{8}$$

For typical axial detector temperatures of $\langle T_z \rangle = 6(2)\,\mathrm{K}$ a modified cyclotron measurement results in an average energy of $\langle E_+ \rangle \approx k_B \cdot 270\,\mathrm{K}$ and $\langle E_- \rangle \approx k_B \cdot 0.1\,\mathrm{K}$ after the sideband coupling.

3. Continuous Stern-Gerlach effect and double trap method

The Larmor frequency ν_L is proportional to the energy that is needed to change the spin state in a magnetic field. A measurement of the spin transition rate as a function of the frequency of an external spin-flip driving field yields the Larmor frequency. To determine the spin state the so-called continuous Stern-Gerlach effect [10] is used which couples the spin state to the axial motion in the presence of a magnetic inhomogeneity called "magnetic bottle", which is deliberately superimposed on the trap. The magnetic bottle adds $V_m = -\mu_z B_z$ to the electric potential energy, which results in a modified axial frequency

$$\tilde{\nu}_z = \frac{1}{2\pi}\sqrt{\frac{2qC_2V_0}{m} \pm \frac{2\mu_z B_2}{m}} \approx \nu_z \pm \frac{1}{4\pi^2}\frac{\mu_z B_2}{m\nu_z} \,. \tag{9}$$

This allows the determination of the spin state by measuring the axial frequency. Here B_2 describes the strength of the magnetic bottle according to $B_z = B_0 + B_2 z^2$. The observable axial frequency change is then given by

$$\Delta\nu_{z,\,SF} \approx \frac{1}{2\pi^2}\frac{\mu_z B_2}{m\nu_z} \approx 170\,\text{mHz} \,. \tag{10}$$

Since μ_z and m are fixed by the particle species, and also ν_z is fixed by experimental constraints, only B_2 can be used to change the size of this frequency jump. In our experiment we use a magnetic bottle with $B_2 = 300\,000\,\text{Tm}^{-2}$ resulting in a jump of 170 mHz at an axial frequency of 750 kHz. The magnetic bottle also couples the cyclotron energy E_+ to the axial motion, being one of the main challenges for spin state detection. As a result, the axial frequency shifts by

$$\Delta\nu_{z,\,n_+\to n_+\pm1} = \frac{1}{2\pi}\frac{\hbar\nu_+}{m\nu_z}\frac{B_2}{B_0} \approx 60\,\text{mHz} \tag{11}$$

each time the cyclotron quantum number changes by $\Delta n_+ = 1$. The rate p_+ of these changes scales linearly as indicated by Fig. 3. (b) with the absolute quantum number n_+ or equivalently, the energy of the cyclotron motion which can be calculated by perturbation theory and the corresponding matrix element [11]. Figure 3. (a) shows a sequence of simulated axial frequency measurements. In the presence of cyclotron quantum jumps the spin-flip can only be observed in case of a low cyclotron energy.

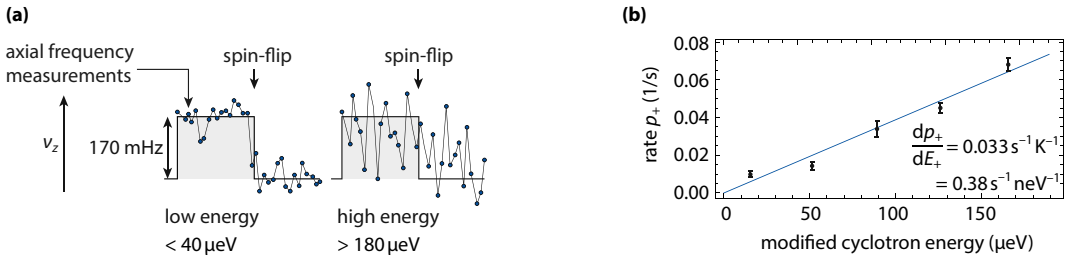

Fig. 3. (a) Using the continuous Stern-Gerlach effect the spin state is coupled to the axial motion. This results in a discrete frequency change of the axial motion due to a spin-flip. The ability to detect such a spin-flip by successive frequency measurements (dots represent simulated data) is limited by the amount of background noise which is a result of the energy fluctuations in the cyclotron motion. The left side shows a particle with low cyclotron energy and the underlying spin-flip is observable, while in case of high cyclotron energy on the right side one cannot conclude that a spin-flip has occurred. (b) The rate p_+ at which cyclotron quantum jumps occur increases with the energy of the particle's modified cyclotron motion.

While a large magnetic bottle B_2 is essential for the determination of the spin state, it leads to systematic shifts of the measured motional frequencies. In our case, the magnetic bottle would limit the precision of the g-factor measurement at the p.p.m. level, if we carried out all frequency measurements and the spin state determination in a single trap. For that reason the double Penning-trap method [5] is used, which utilizes two traps as shown in Fig. 4. The so-called precision trap (PT) is used to carry out precise frequency measurements and to drive spin-flips. The second trap is the analysis trap (AT) with the strong magnetic bottle superimposed to identify the spin state. Due to the spatial separation the magnetic field in the PT of the previous setup was by a factor of around 75 000 times more homogeneous than in the AT. This allows measurements at the p.p.b. level.

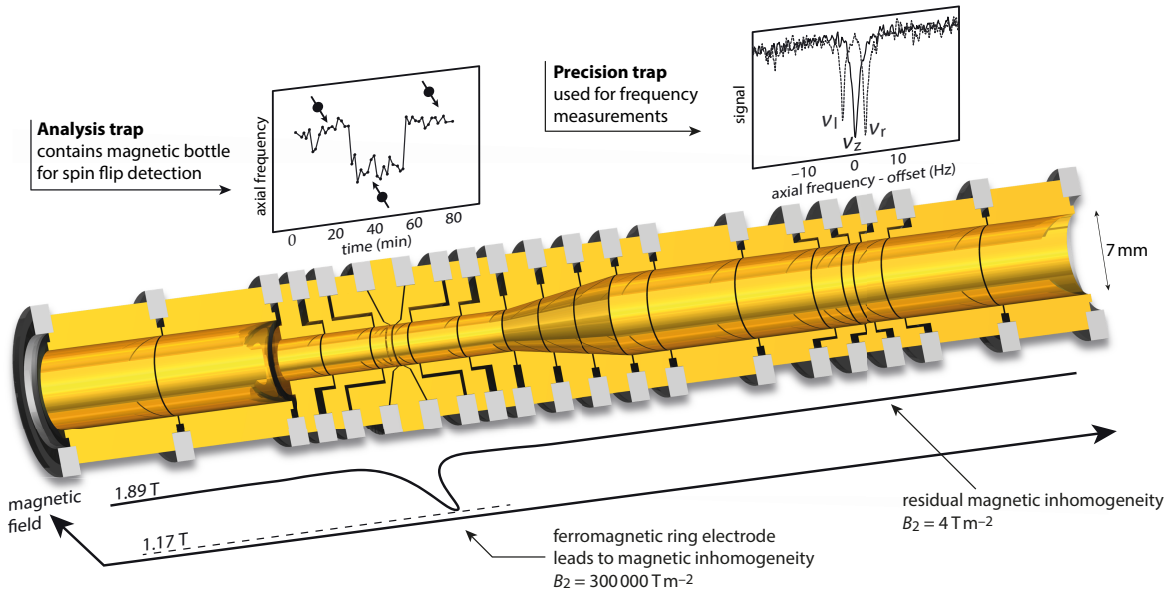

Fig. 4. The double trap of the Mainz g-factor proton experiment with the analysis trap (AT) for the spin state detection and the precision trap (PT) for precise frequency determination.

For the g-factor measurement in the double trap scheme, the proton starts in the AT where the spin state is detected. After moving to the PT, the free cyclotron frequency is measured. At the same time a test frequency is applied close to the Larmor frequency to induce a spin-flip. Since free cyclotron frequency measurement and the Larmor drive are carried out at the same time the magnetic field cancels in the frequency ratio. Finally, the proton is once again transported to the AT where the spin state is measured a second time. Together with the first spin state measurement, this determines whether or not a spin-flip occurred in the PT. The process is repeated several hundred times for different test frequencies in the PT. The resulting Larmor resonance from all test frequencies together with the free cyclotron frequency measurements is then used to determine g.

4. Towards sub-p.p.b. precision

To improve the measurements to the sub-p.p.b. level careful analysis of the main limitations in our last g-factor measurement from 2014 is required. In this section we will discuss how the width of the g-factor resonance can be decreased by reducing the magnetic inhomogeneity in the PT and by reducing fluctuations of the magnetic field. Furthermore, particle preparation can be made more efficient. This reduces the measurement time per data-point and thus improves statistics.

After a double-dip measurement the measured values of the modified cyclotron energy are exponentially distributed. The energy can be measured in the AT since the axial frequency is a function of the cyclotron energy in the presence of the magnetic bottle. The coupling of E_+ to the axial frequency in the presence of the residual magnetic bottle in the PT induces line shape broadening. In order to reduce B_2 the distance between the PT and the AT was increased while keeping the total length of the trap assembly constant. This corresponds to a decrease in $B_2 = 0.5\,\mathrm{Tm}^{-2}$, which is a factor of 8 smaller than in the 2014 measurement.

Other limitations to the cyclotron frequency stability are magnetic field fluctuations. For that reason a self-shielding coil [12] was implemented with its highest shielding in the center of the PT. Such a coil keeps the surrounding magnetic field flux constant and cancels external magnetic field fluctuations. Our coil reduces magnetic field disturbances along the trap axis by around a factor of 50. Figure 5. shows the combined result of B_2 reduction and installed shielding coil and thus improved short term stability. Compared to the previous run the cyclotron stability was improved by a factor of 10, therefore enabling g-factor measurements below the p.p.b. level.

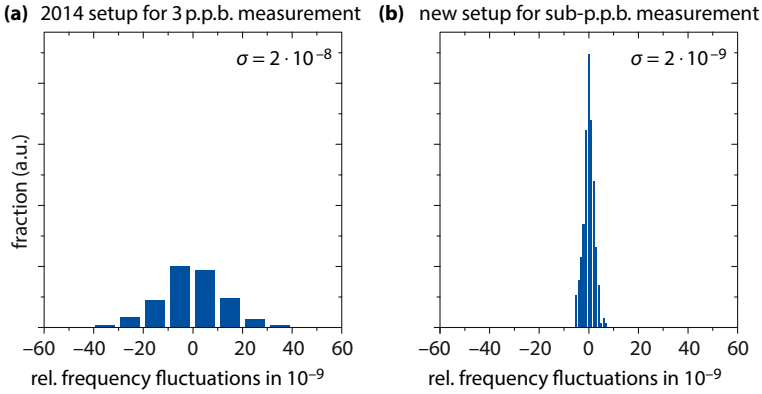

Fig. 5. (a) shows the cyclotron stability for the measurement in 2014 while (b) shows the result for the new setup with smaller residual magnetic field in the PT and the self-shielding coil installed. The improvements allow an increase of the g-factor's measurement precision by at least one order of magnitude.

Independent measurements of the axial stability show that the width of the cyclotron stability can be explained solely by voltage fluctuations, since the modified cyclotron frequency is measured by coupling to the axial mode. The stability is thus not limited by external magnetic field fluctuations or coupling effects due to B_2. To improve the cyclotron frequency stability further using the double-dip technique, a stabilization of the axial frequency by developing improved power supplies for example based on Josephson voltage references is required. Alternatively, a direct measurement of the modified cyclotron frequency could be implemented, for example by using phase-sensitive detection techniques [13, 14, 15].

Due to the scaling of the axial frequency stability with the cyclotron quantum number n_+, a low cyclotron energy (typically $E_+/k_\mathrm{B} < 1\,\mathrm{K}$) is a crucial requirement for spin state detection. However, each measurement of the modified cyclotron frequency raises the energy of the mode drastically (typically $E_+/k_\mathrm{B} \approx 200\,\mathrm{K}$) and the cyclotron energy needs to be reduced after each individual measurement of ν_+. This is achieved by tuning the cyclotron resonator to the modified cyclotron frequency of the proton. The resonator then acts as a thermal bath at a temperature T_res [16], similar to the axial detector in case of the axial mode. When the proton is decoupled from the thermal bath it acquires a fixed but arbitrary cyclotron energy. The distribution of the individual energy values follows an exponential distribution, its width being defined by the thermodynamic temperature. To prepare a single

proton which meets the requirements of spin state detection it is repeatedly coupled to the resonator until it is found in the lowest temperature bin.

In our 2014 measurement this particle preparation time was around 100 minutes out of the 160 minutes for the entire measurement cycle and therefore was a major contribution to the time budget of the measurement [3]. The preparation time is set by the temperature of the resonator T_{res} ($\sim$ number of required cycles) and the coupling constant t_{cpl} ($\sim$ time per cycle). So improving either of these would decrease the particle preparation time significantly.

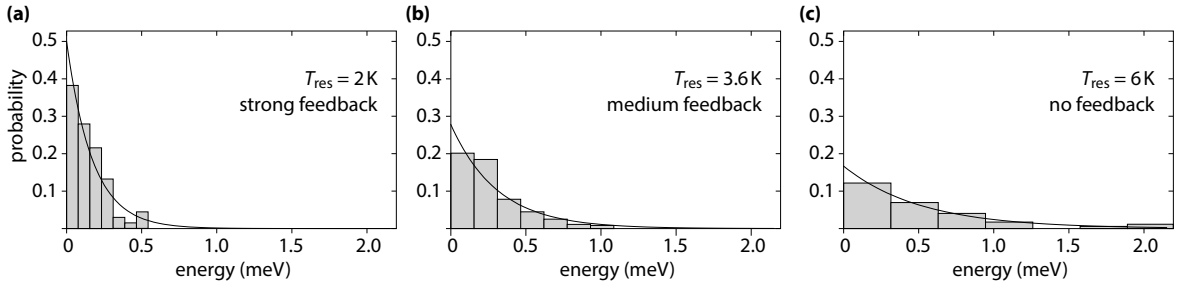

Fig. 6. The proton is coupled to a cyclotron resonator with temperature T_{res}. After waiting for a time t_{cpl} the particle is in one of the bins according to the Boltzmann distributed probability. By using active electronic feedback the effective temperature of the detector can be reduced. (a) represents the coldest achievable temperature for the cyclotron detector with active feedback.

For that reason a new superconducting resonator at 28.9 MHz was built, with a quality factor $Q = \nu_0/\Delta\nu = 1400$ with the resonator frequency ν_0 and the full width at half maximum $\Delta\nu$. Through active electronic feedback [17, 18] the actual temperature of the detector can be decreased to $T_{\mathrm{res}} = 2\,\mathrm{K}$, compared to $T_{\mathrm{res,old}} = 5\,\mathrm{K}$ for the previously used cyclotron resonator with feedback in 2014 [19]. Figure 6. (a)-(c) shows three temperature measurements with and without feedback. Hereby the proton is coupled to the thermal bath and its energy is measured subsequently. Repeating this for several times one obtains a Boltzmann distribution which characterizes the thermal bath and thus the temperature of the cyclotron detector. Besides the improved temperature also the coupling time constant of the new cyclotron detector is by a factor of 2 better with $t_{\mathrm{cpl}} = 60\,\mathrm{s}$, compared to $t_{\mathrm{cpl}} = 120\,\mathrm{s}$ of the previous one. In total the new detector allows a factor of four times faster particle preparation that reduces the total measurement cycle time by a factor of two which doubles the amount of accumulated data within the same time window.

5. Conclusion

The goal of our experiment is to measure the g-factor of the proton at the sub-p.p.b. level. Since the previous measurement in 2014 with a relative precision of 3.3 p.p.b. several upgrades have been made, including a smaller residual magnetic field inhomogeneity in the precision trap, the installation of a self shielding coil and the implementation of a new cyclotron detector for faster particle preparation. These optimizations should allow to improve the previous result by around one order of magnitude.

In the future, these techniques can be applied to the antiproton, providing a stringent sub-p.p.b. test of CPT symmetry.

Acknowledgment

We acknowledge financial support by the RIKEN Initiative Research Unit Program, RIKEN President Funding, RIKEN Pioneering Project Funding, RIKEN FPR Funding, the RIKEN JRA Program,

the Grant-in-Aid for Specially Promoted Research (grant number 24000008) of MEXT, the Max-Planck Society, the EU (ERC advanced grant number 290870-MEFUCO), the BMBF, the Helmholtz-Gemeinschaft, and the CERN Fellowship programme.

References

[1] C. Smorra *et al.*, Eur. Phys. J.-Spec. Top **224**, 3055 (2015)
[2] S. Ulmer *et al.*, Nature **524**, 196 (2015)
[3] A. Mooser *et al.*, Nature **509**, 596, (2014)
[4] P. F. Winkler *et al.*, Phys. Rev. A **5**, 83 (1972)
[5] A. Mooser *et al.*, Phys. Lett. B **723**, 78 (2013)
[6] S. Ulmer *et al.*, Phys. Rev. Lett. **106**, 253001 (2011)
[7] G. Gabrielse *et al.*, Int. J. Mass Spectrom. Ion Processes **88**, 319 (1989)
[8] L. S. Brown *et al.*, Rev. Mod. Phys. **58**, 233 (1986)
[9] L. S. Brown *et al.*, Phys. Rev. A **25**, 2423 (1982)
[10] H. Dehmelt *et al.*, Bull. Am. Phys. Soc. **18**, 72 (1973)
[11] A. Mooser *et al.*, Phys. Rev. Lett. **110**, 140405 (2013)
[12] G. Gabrielse *et al.*, J. Appl. Phys. **63**, 5143 (1988)
[13] J. K. Thompson *et al.*, Nature **430**, 58 (2004)
[14] S. Rainville *et al.*, Science **303**, 334 (2004)
[15] S. Sturm *et al.*, Phys. Rev. Lett. **107**, 143003 (2011)
[16] S. Djekic *et al.*, Eur. Phys. J. D. **31**, 451 (2004)
[17] H. Dehmelt *et al.*, Proc. Nat. Acad. Sci. **83**, 5761 (1986)
[18] B. d'Urso *et al.*, Phys. Rev. Lett. **90**, 43001 (2003)
[19] S. Ulmer *et al.*, Rev. Sci. Instrum. **80**, 123302 (2009)